EE152: Radio Final Project

Devin Cody and Dan Jamison

October 16, 2018

Abstract

In this report, we describe the results of the design and testing of a 5.8 GHz radio and its subsystems. The objective of this project is to create the longest link between a transmit (TX) device and a receive (RX) device possible. In the construction of this radio, we built and optimized four microwave components including a balanced mixer, an oscillator, a band-pass filter, and a patch antenna array. In the end, our system achieved a link distance of over 250 feet while having a signal to noise ratio of over 70dB.

1 Introduction

1.1 Radio Theory of Operation

Typical FM radios work on the principal of up-conversion whereby a mixing circuit takes a low frequency audio signal (20Hz - 20kHz) and a local oscillator circuit (usually between 88 and 108 MHz) and mixes the audio signal up to the frequency of the local oscillator. This signal is then amplified many times, transmitted, and received using any common radio receiver. Internal to most common radio receivers is a mixer which down converts the high-frequency RF signal into the audio band — a process which completely reverses the up-conversion step preformed at the start of the process.

The double conversion radio is very similar to the single conversion radio, however, the double conversion radio utilizes 2 cascaded mixing stages that allows mixing to higher frequencies and with more accuracy than a single mixing stage. We will use double conversion in this project to generate our radio signal.

1.2 System Design

The basic block diagram of our system is shown in Figure 1. In this project, we will be using a commercial off-the-shelf (COTS) radio tuner to generate an FM signal at approximately 100MHz then up-converting a second time with an oscillator at 5.8GHz. The radio tuner component is represented in both the TX and RX sub-systems as a digital to analog converter (DAC) with mixer and local oscillator in a dashed box. After generating the FM signal, we subsequently up-convert our signal to roughly 5.9 Ghz. The up-conversion processes relies on a custom mixer based on dual Schottky diodes and a custom oscillator based on the BFU730 transistor. The amplifier between the mixer and the oscillator is important to desensitize the oscillator to the impedance discontinuity at the mixer input. Next, we remove the harmonics of the mixer with a custom 5-element distributed element filter. Finally, we pass our signal through a series of three amplifiers which have been selected to provide large amounts of amplification and a high 1dB compression point such that we can drive our antennas with the maximum amount of power possible (roughly 20dB in theory).

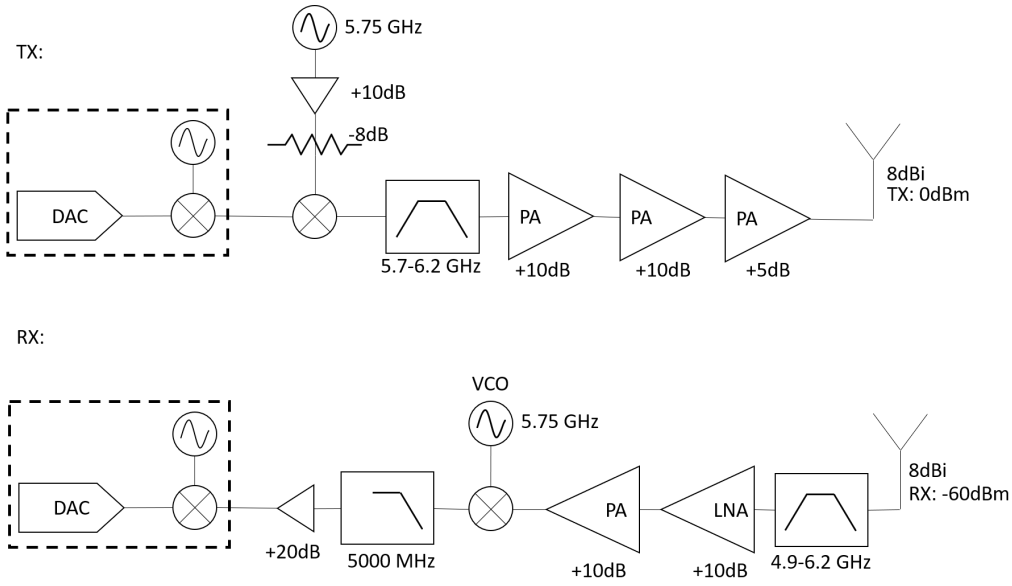

Figure 1: Block diagram of our implemented radio system. Boxes with dashed lines represent the FM transmitter and receiver.

On both the transmit (TX) and receive (RX) subsystems, we are using 4-element patch array antennas. This antenna topology gives us significant directivity ($\sim$ 8.4dBi) and will allow us to transmit over a farther distance compared to a single patch antenna or a cantenna.

The RX subsystem is very similar to our TX system. The RX system starts with another 4-element patch antenna array which is immediately connected to a 5.8GHz BPF which prevents our amplifiers from saturating with other ambient noise. We follow the band pass filter with a low noise amplifier and then a common amplifier which will further bump up our signal. Next, we down-convert our signal from 5.8GHz down to the FM radio band with a voltage-controlled oscillator (VCO) and custom mixer. Finally, we amplify our signal one last time in the FM band before using the COTS radio to read our signal.

2 Design and Characterization

Before any of the systems were pieced together, each of the components was tested individually to ensure that their functionality was as expected and the frequencies of operation matched those of the design.

2.1 Antennas

To maximize the distance over which we could transmit, we decided to design and build a patch antenna array consisting of 4 elements. We started by designing a single patch antenna which was designed and optimized using the electromagnetic simulator, CST. The initial design followed the equations presented in Casu et al.[1], however the design was subsequently optimized to obtain the smalled S11 reflection coefficient over the frequency range 5.7-5.9GHz. The directivity of this simulated antenna was 4.3dBi at 5.8GHz and had a FWHM beam-width almost 120 degrees as shown in Figure 3.

[1]http://ieeexplore.ieee.org/stamp/stamp.jsp?arnumber=6866738

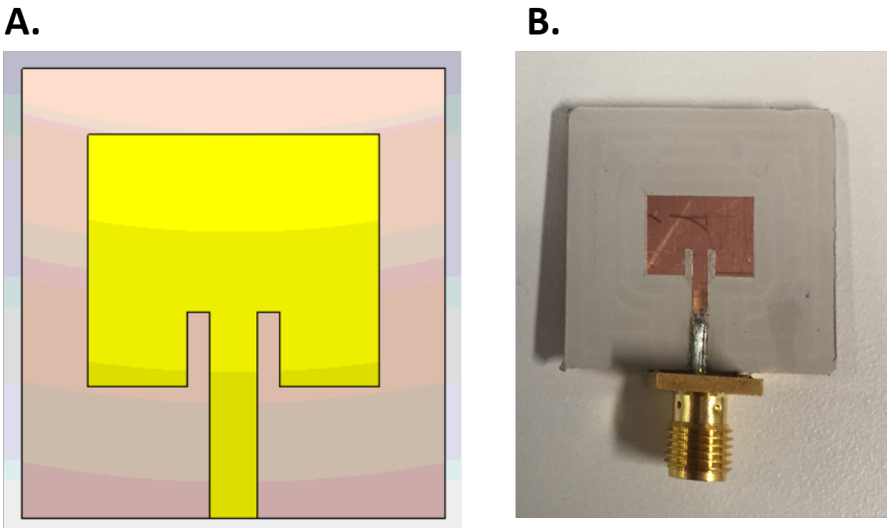

Figure 2: Patch antenna as simulated in CST (A). Patch antenna as fabricated (B).

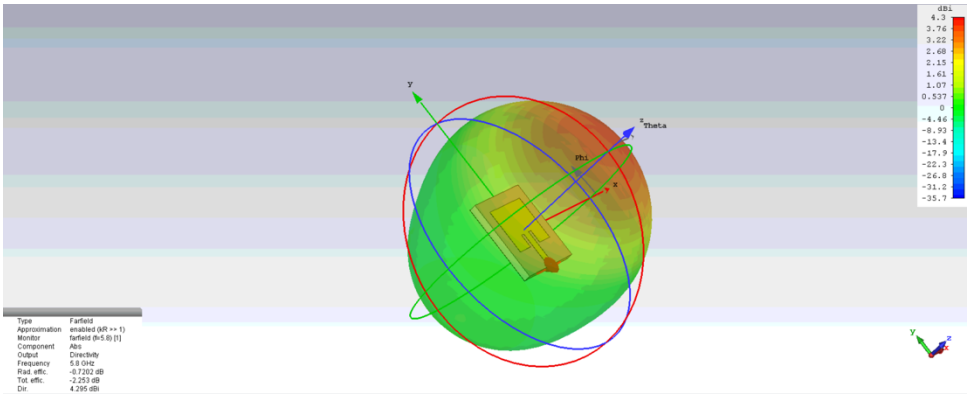

Figure 3: Radiation pattern of a single patch antenna at 5.8GHz.

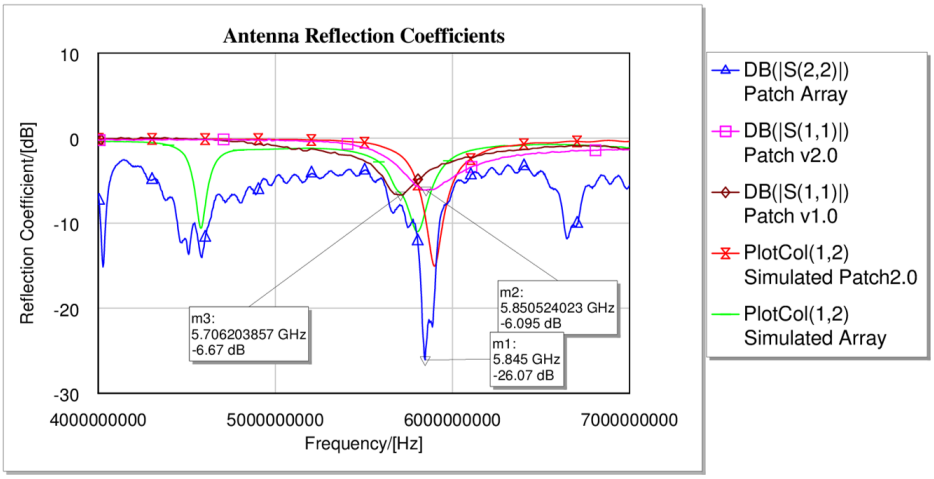

Figure 4: Reflection coefficients for the various antenna topologies.

Once the design was optimized in CST, we fabricated the antenna and measured the reflection coefficient to compare the result to simulation. Figure2 shows the antenna as it was simulated int CST (A) and as it was fabricated (B). Although the patch was simulated with a resonance at 5.8GHz, the fabricated antenna's reflection coefficient got detuned by about 100MHz. This is shown in Figure 4. The fabricated antenna's S11 is shown in the brown line. To compensate, we designed a second patch antenna in CST (patch v2.0, red line) that was tuned up in frequency by 100MHz. Once this second antenna was fabricated (pink line), the resonant frequency was correctly located at $\sim 5.8GHz$.

Finally, we designed a 4-element patch array antenna in CST and optimized the design to maximize the directivity of our antenna. The antenna array design can be seen in Figure 5. The design of this antenna is largely dependent on 3 two-way splitters where a 50 ohm trace is split into two 100 ohm traces and the power is divided evenly[2]. Simulations of the antenna far field pattern (Figure 6) show a directivity of 11.4dBi which would beat the directivity of any cantenna. The FWHM beam-width was roughly 50 degrees.

Reflection coefficient measurements of the fabricated array show that the fabricated array has a smaller reflection coefficient than the simulated version (see blue and green lines in figure 4).

2.1.1 Gain Calculations

For calculating the power received by an antenna, P_{RX} we use the formula:

$$P_{RX} = \frac{G^2\lambda^2}{(4\pi R)^2} P_{TX}, \tag{1}$$

where P_{TX} is the transmitted power, G is the gain, λ is the design wavelength, and R is the distance between the antennas. Solving this equation for the gain of the antennas, we find

$$G = \frac{\nu 4\pi R}{c} \sqrt{\frac{P_{RX}}{P_{TX}}}, \tag{2}$$

[2]For an example of the perils of 100ohm traces see Figure 36.

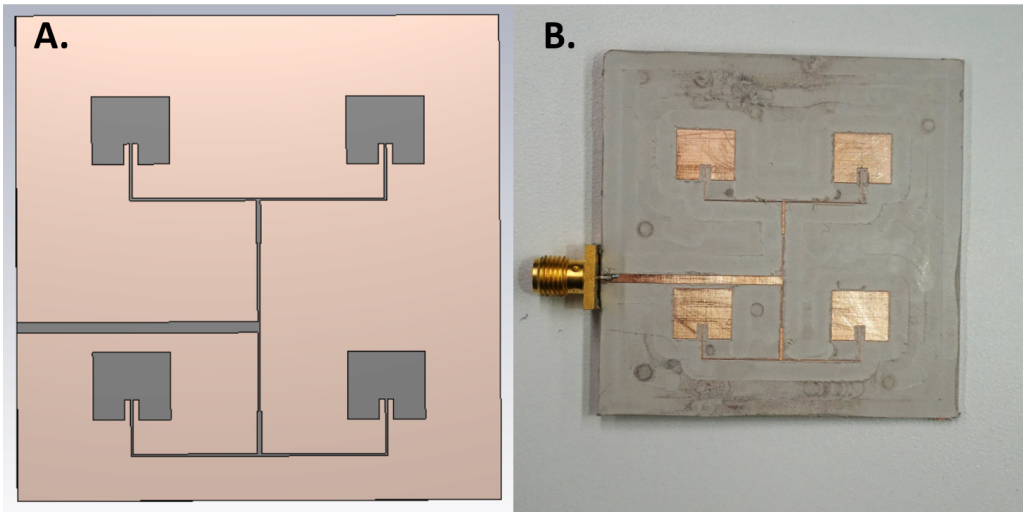

Figure 5: Patch array as simulated in CST (A) and as fabricated (B).

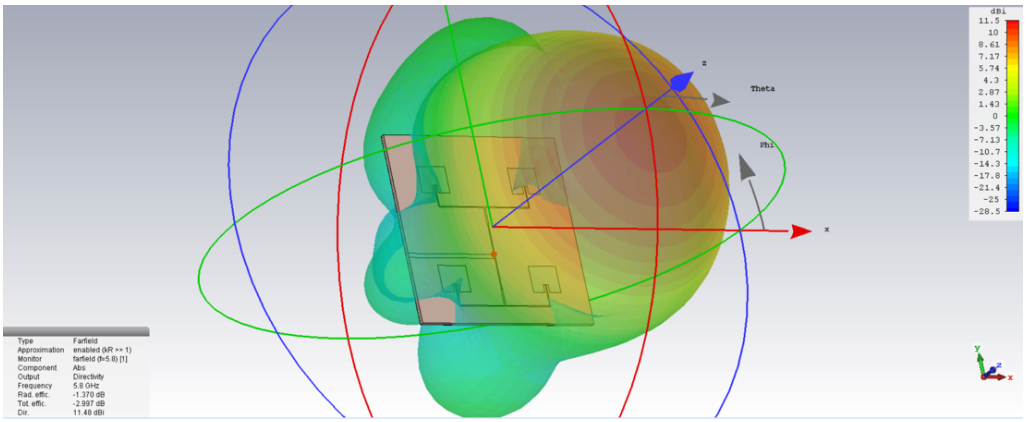

Figure 6: Radiation pattern of the optimized 4-element patch antenna array. Directivity is 11.4dBi.

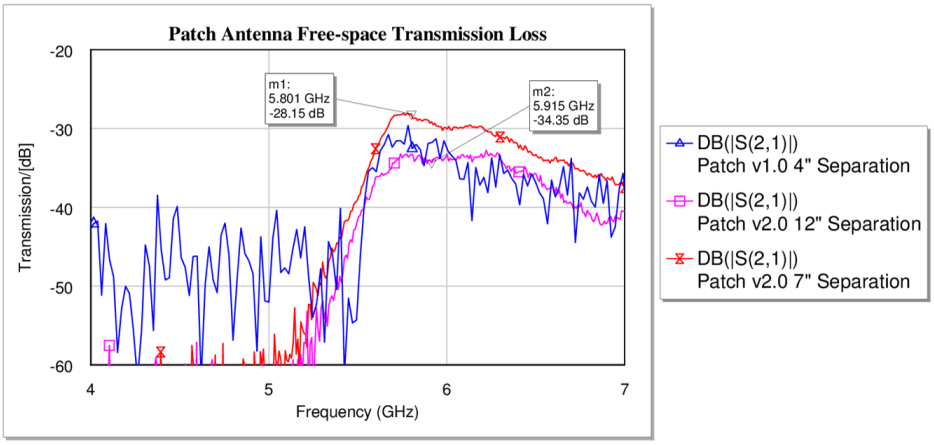

Figure 7: S21 and S12 measurements for a set of patch antennas at different distances.

where ν is the frequency of operation assuming a relative dielectric constant of $\epsilon_r = 1$ and c is the speed of light. Converting Equation (2) to dB:

$$G_{dBi} = 10\log_{10}\left(\nu\frac{4\pi R}{c}\right) + \frac{1}{2}[P_{RX} - P_{TX}] \tag{3}$$

The setup for the antenna gain measurement included two identical antennas (patch or array) connected to the Field Fox VNA. We set the transmit power to 0dBm and then took s21/S12 measurements. Figures 7 and 8 show the S21 measurements for the patch antennas and the antenna arrays respectively.

Therefore we observe the following gain measurements for the patch and array antennas:

$$G_{dBipatch} = 10\log_{10}\left(5.8\times10^{9}Hz\frac{4\pi 12in}{3\times10^{8}m/s}\right) + \frac{1}{2}[-34.35] = 1.02dBi$$

$$G_{dBiarray} = 10\log_{10}\left(5.8\times10^{9}Hz\frac{4\pi 19in}{3\times10^{8}m/s}\right) + \frac{1}{2}[-24.52] = 8.43dBi$$

Clearly, the patch antenna array demonstrates superior directivity.

2.2 Coupled-line Band Pass Filter

One commonly implemented distributed element filter is the hair-pin filter. This filter is very similar to the traditional parallel-coupled lines filter, however, here, the lines are bent such that the overall topology is more compact. We started by designing a 3-segment filter but then quickly moved to 5 and 7-segment filters (See Figures 28, 29, and 30 respectively). This design choice was made to maximize the steepness of the cut-off region and reduce the bandwidth of the pass-band — ideally to our operating frequencies of 5.7-5.9GHz.

The starting point for our design was a 3-segment topology demonstrated by a report by Peter Martin[3] which was subsequently optimized for use at 5.8GHz, adapted into 5- and 7-segment topologies, and then throughly optimized in microwave office.

The final layouts for the circuits are shown in Figure 11(ABC) The 7-segment section obtained a bandwidth of 5.65 to 5.95GHz while the 5-segment filter was optimized to have a bandwidth

[3]https://awrcorp.com/download/kb.aspx?file=appnotes/EC_Mstrip_BPFilter.pdf

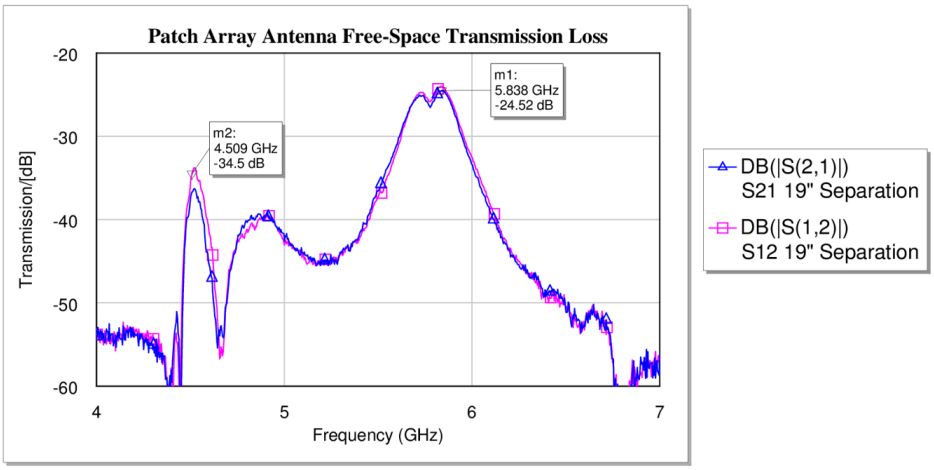

Figure 8: S21 and S12 measurements for a set of patch antenna arrays at different distances.

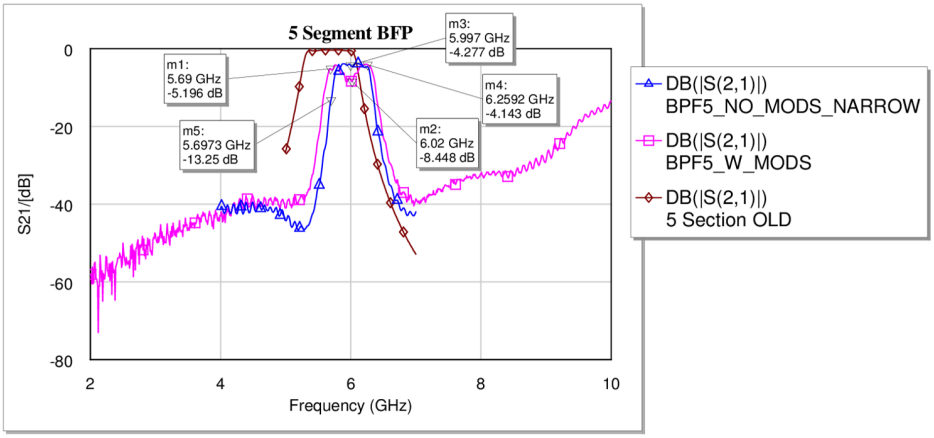

Figure 9: Simulated (brown) and measured (blue) S21 parameters for a 5-segment band pass filter. Pink trace shows measured s21 after modifications were made to extend the bandwidth.

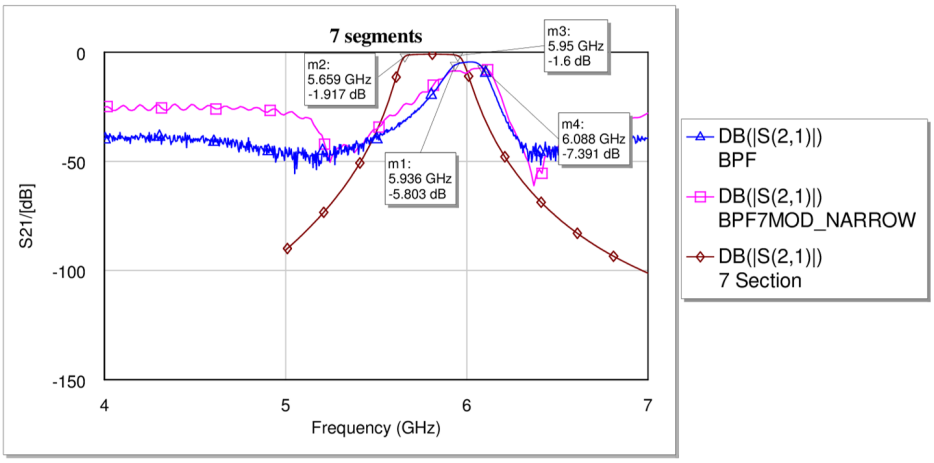

Figure 10: Simulated (brown) and measured (blue) S21 parameters for a 7-segment band pass filter. Pink trace shows measured s21 after modifications were made to extend the bandwidth.

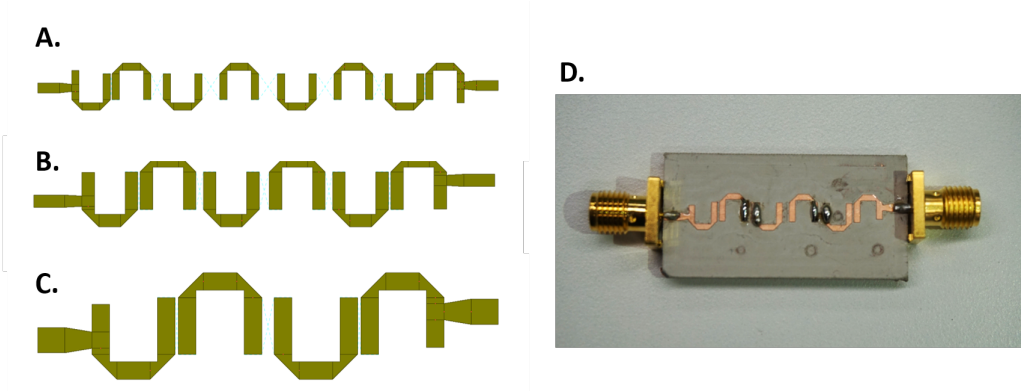

Figure 11: Layouts for the 3-segment BPF (A), 5-segment BPF (B), and 7-segment BPF (C). Example of a fabricated circuit (5-segment) which has been modified to make the bandwidth wider(D).

of about 700MHz from 5.3 to 6.0GHz, as shown in brown traces in Figures10 and 9 respectively. Before deciding on either design in our project, we fabricated both the 5-segment and the 7-segment designs to see which one would be the better fit. The S21 parameters for the measured BPF are shown in the blue traces in Figures 9 and 10. Here it's clear that both of the designs were tuned up in frequency by almost 300MHz and there was significant loss even in the band-pass regions. Although it's not entirely clear what caused this detuning, simulations in microwave office reveal that it's possible to recreate the frequency detuning by making all the traces longer or by decreasing the dielectric constant. As for the discrepancy in pass-band loss, we attribute this to a combination of the dielectric loss tangent (.0027 for rogers 3210) which contributes $\sim 1dB$ and losses due to the large gaps between the coupled transmission lines which might add another 2dB.

Regardless, It was imperative that we not lose our signal over the design frequency so effort was needed to shift the frequencies of operation down to the 5.7 to 5.9GHz band. Through a combination of experimentation in MWO and on the physical filter we discovered that by enhancing the coupling between the 2nd and 3rd transmission line segments, we could effectively increase the bandwidth of the filter such that it would correctly span the lower frequencies in our band of operation. The coupling was enhanced by pooling solder on the aforementioned coupled section of the transmission line (and their symmetric pairs). A modified 5-segment BPF is shown in Figure 11D. The result was a band pass filter with additional ripple in the pass band, but a more suitable bandwidth. The final [S] parameters of our circuit can be seen in the pink lines in Figures 9 and 10.

2.3 Mixer

Another important component of our circuit was the mixer. Mixers are useful devices which allow us to exploit non-linearities in a predictable fashion and convert between frequencies. For our mixer, we used a hybrid mixer topology consisting of a branchline coupler and dual mixing Schottky diodes. From a theoretical standpoint, these mixers utilize these diodes and a powerful local oscillator (LO) to act as a switch for an RF signal. In effect, this switching action multiplies the RF signal by square-wave signal at the LO frequency. In the frequency domain, this is equivalent to a convolution of the RF signal spectrum with the odd-multiples of the LO frequency as produced by the square wave. The final result is that we can shift the RF signal to any frequency by using an appropriate LO tone.

The circuit used in this project is identical to the one described previously[4], but it summarized here for completeness. The design of the mixer started by developing an equivalent circuit for the diodes which will improved our ability to develop matching circuits. Next, we added and optimized open radial stubs to reduce the LO signal from leaking out of the IF port. Finally, we added all the sub-circuits together and optimized for impedance match.

In Lab 4 we measured the conversion loss as a function of various parameters such as RF frequency, LO input power, or RF input power as reproduced in Figure 13 . However, in all of these measurements, signals were injected on the RF and LO ports and the low frequency IF port was used as an output. However, in our radio application, we are interested in using the IF port in the RX chain as an output (for down-conversion) and as an input in the TX chain(for up-conversion). To better understand the conversion loss of the mixer in up-conversion applications, several conversion loss measurements were made as shown in Figure 14. For up-conversion, the conversion loss bottoms out at around 15dB for all the tests that we did. This happens with an LO power of greater than +2dBm and an IF Power of less than -5dBm. For down-conversion, the conversion loss bottoms out at around 10dB for all the tests that we did in lab 4. The optimimum conversion loss happens for LO inputs of great than 4dBm and for RF inputs of less than -10dBm.

[4]See Cody and Jamison, Lab 4, 2017

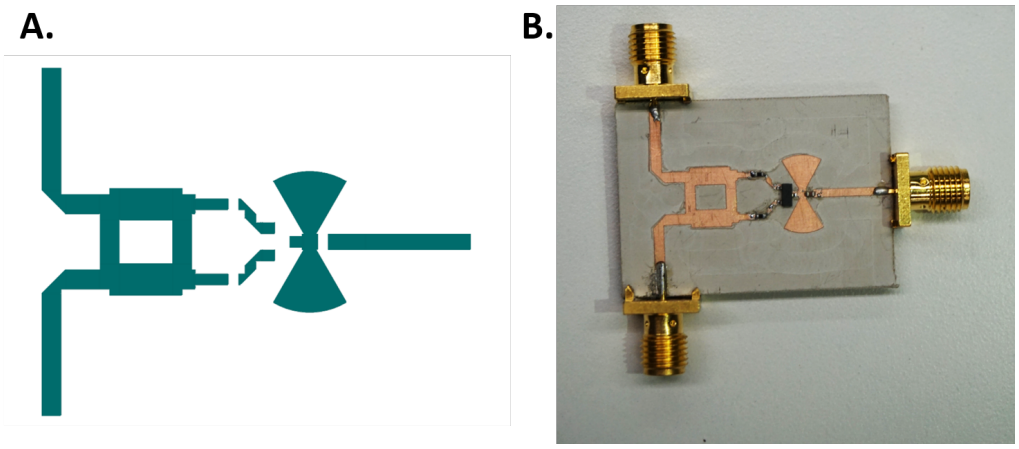

Figure 12: Layout of mixer circuit as designed int MWO (A) and mixer circuit as fabricated and assembled (B).

2.4 Oscillator

The other custom active component that we developed was a 5.8GHz Oscillator for converting our FM band signal to 5.8GHz. Again this component was first developed in lab 6[5], but we will briefly recapitulate its design.

2.4.1 Oscillator Biasing

The Oscillator biasing network was implemented as discussed in the lab handout. We first converted all of the .S2P files into .S3P files using the code shown in the Appendix. The transformation which the code implements can be found in the lab 6 handout.

We then developed a test bench where we connected a inductive load to the base of our transistor and varied it's value to obtain a minimum stability K-value. This minimum occurred for a bias condition of 2V and 15mA for a stability K-value of -0.9805. We subsequently designed our bias networks to meet these conditions.

Using the datasheet[6] provided by NXP, we find that if we want 15mA collector current, we need to supply $\approx 50\mu A$ of current on the transistor base. Given a supply voltage of 2.15V and a V_{BE} from the datasheet of .8104V, we find that the resistance needed in the base biasing arm of the oscillator is:

$$\frac{V_{CC} - V_{BE}}{50\mu A} = \frac{1.339}{.00005} = 26k\Omega.$$

Additionally, to bias the collector network we have:

$$\frac{V_{CC} - V_{CE}}{15mA} = \frac{0.15}{.015} = 10\Omega.$$

The final biasing circuit can be seen in Figures 31 and 32 (see end of doc).

[5]See Cody and Jamison, Lab 6, 2017
[6]https://www.nxp.com/docs/en/data-sheet/BFU730F.pdf

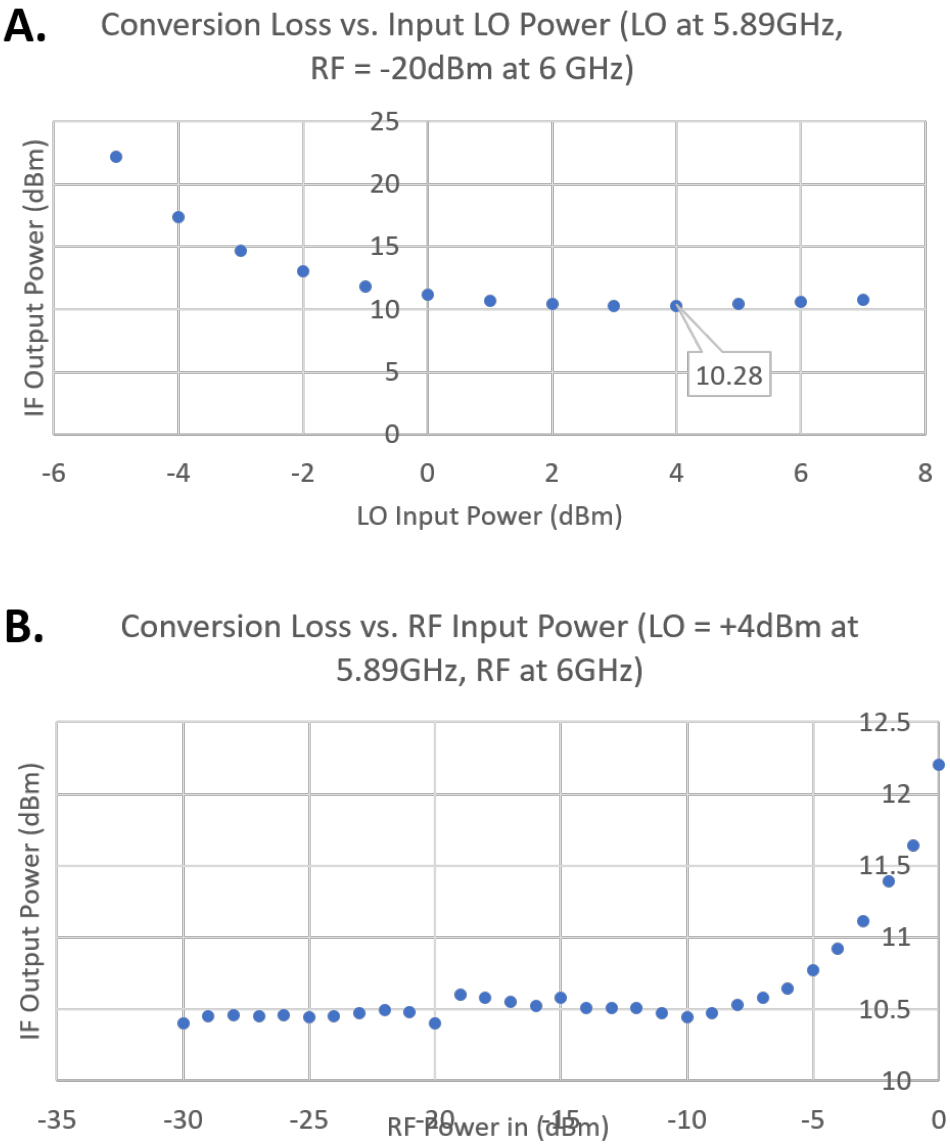

Figure 13: Conversion Loss (from RF to IF) as a function of LO power (A) and as a function of RF power (B) for a downconverting application.

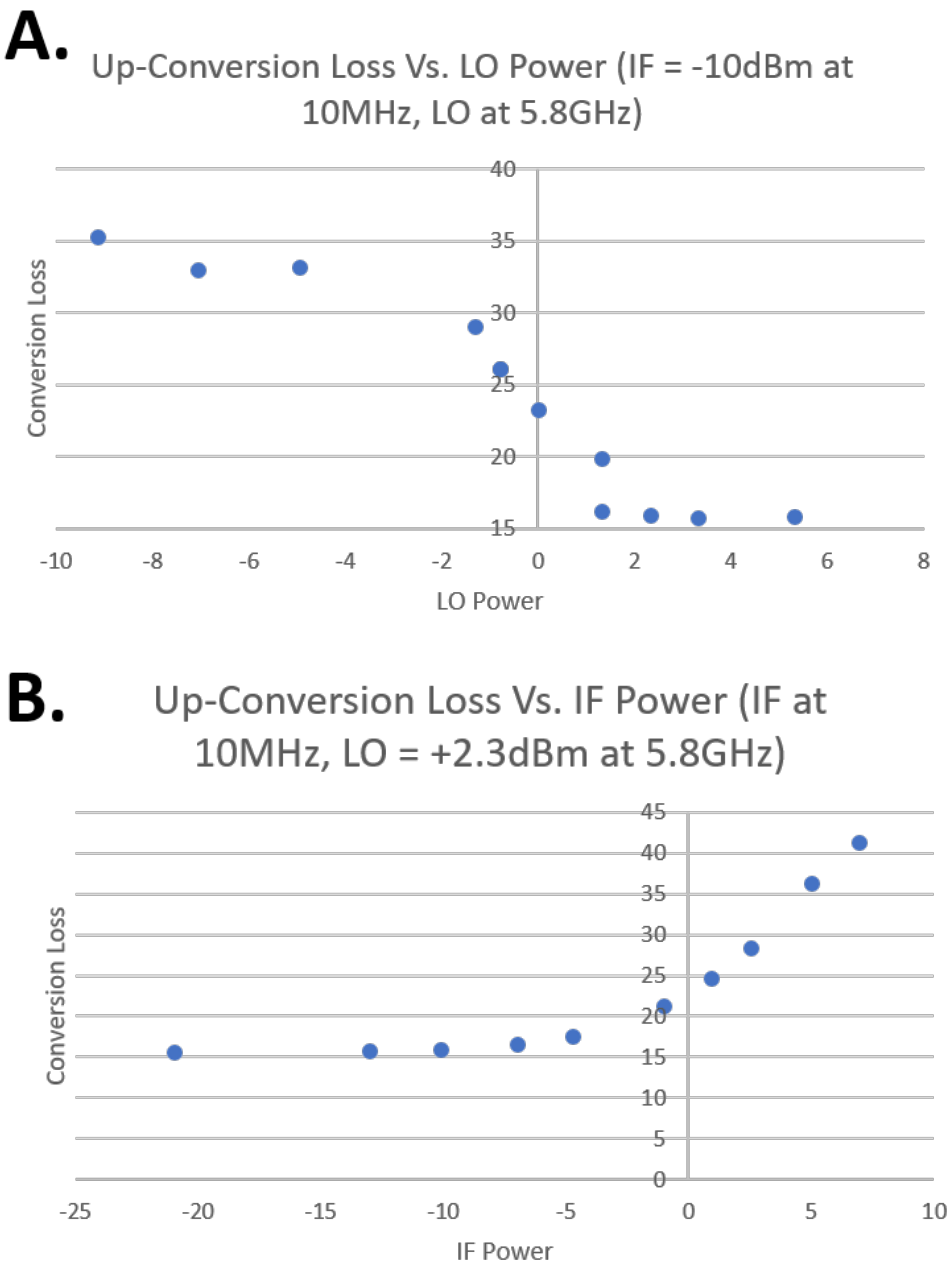

Figure 14: Conversion Loss (from IF to RF) as a function of LO power (A) and as a function of IF power (B) for an upconverting application.

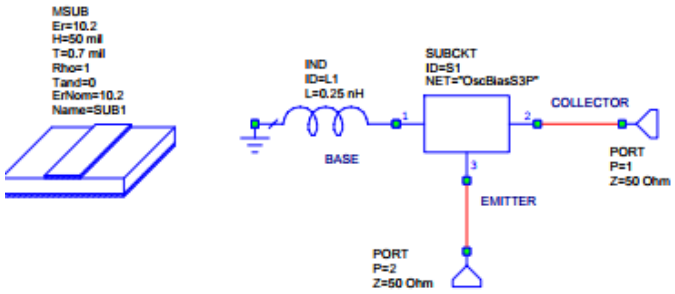

Figure 15: Testing schematic to determine transistor stability factor.

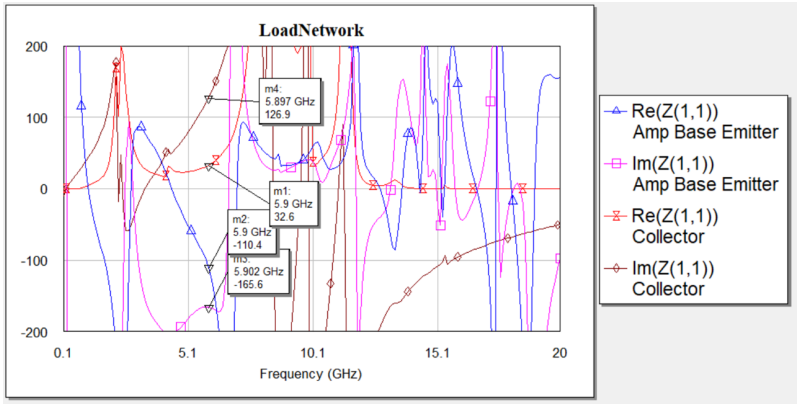

Figure 16: Real and imaginary input impedances for looking into the transistor's collector (Blue and Pink) and for looking into the collector network (red and maroon).

2.5 Output Network Design

The next sub circuit that we designed was the output network which needed to present a 50ohm output and provide a path for DC bias. Effort was made to ensure that the stability of the circuit was kept as low as possible.

2.6 Load Network Design

Lastly, we designed our load network which is the where the feedback for oscillation occurs. The final design is shown in Figure 31. In Figure 16 we optimized the relative impedances of the transistor collector and collector network. Looking into the collector of the transistor, we see negative real and imaginary impedance components which will cause the transistor to oscillate. As discussed in the lab report, we need to bias the collector load network to present an imaginary impedance roughly equal to the magnitude of the negative imaginary impedance looking into the collector of the transistor and a real impedance equal to one third the magnitude of the real impedance of the transistor to ensure oscillation. To accomplish this, we used an inductor and a resistor in the collector network to generate these impedances. The first resistance used was 13 Ω and the first inductor used was 2.0nH. However, as with many microwave technologies, the first attempt is usually wrong. We subsequently spent many hours removing the inductors and resitors until we found a combination that gave us a oscillation frequency of 5.75GHz. Output spectrum of oscillation can be seen in figure 17.

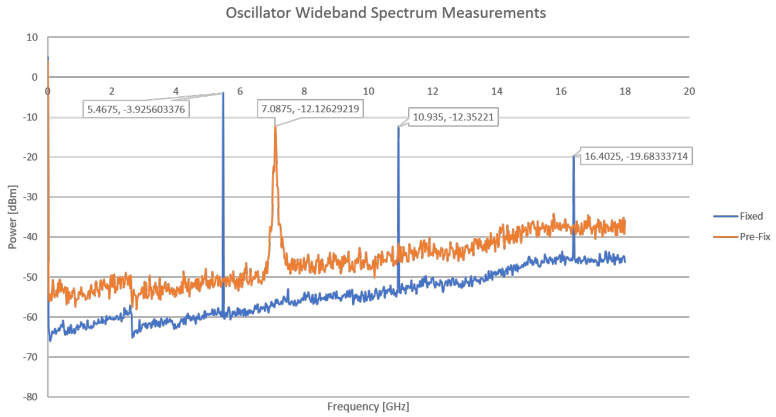

Figure 17: Oscillator Spectrum

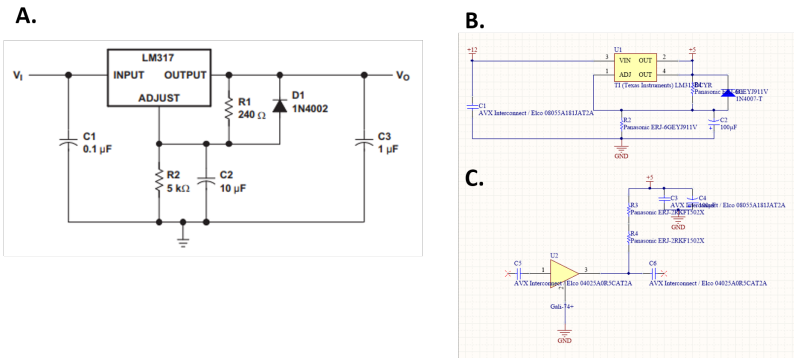

Figure 18: Additional Circuits developed for the radio project. Idealized schematic for a linear regulator circuit (A) Circuit schematic for linear regulator as implemented in PCB tool (B) and circuit schematic for an amplifier board as implemented in a PCB tool (C).

3 Peripheral Components

3.1 Amplifiers

For our project, we selected 3 commercial mmic amplifiers from Mini-Circuits whose specifications most nearly matched our needs. The amplifiers that we identified were the Gali-74+ (for operation from 0 to 1GHz), the Gali-39+ (for low noise applications at 5.8Ghz), and the PHA-1+ (for high power operation at 5.8GHz). The amplifiers were biased as discussed in their data sheets[7][8][9] and PCBs were designed for all of them. The first two amplifiers were biased using the 12 volts from the battery packs while the PHA-1+ used a linear regulator to obtain a bias voltage of 5V. The schematic for the amplifying board is shown in Figure 18C and the layouts are shown in Figure 19C. The schematic for the amplifier board which uses the PHA-1+ and linear regular is shown in Figure 18B and the layout is shown in Figure 19B. The linear regulator schematic and layouts are shown in panels A of the same figures.

[7]https://www.minicircuits.com/pdfs/GALI-74+.pdf
[8]https://www.minicircuits.com/pdfs/GALI-39+.pdf
[9]https://www.minicircuits.com/pdfs/PHA-1+.pdf

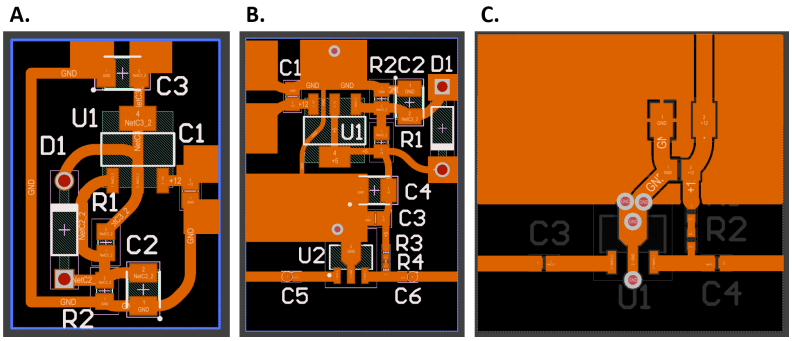

Figure 19: Layout for linear regulating PCB (A) for an amplifier with a 5V voltage regulator on board (B) and for an amplifier biased to 12 volts (C).

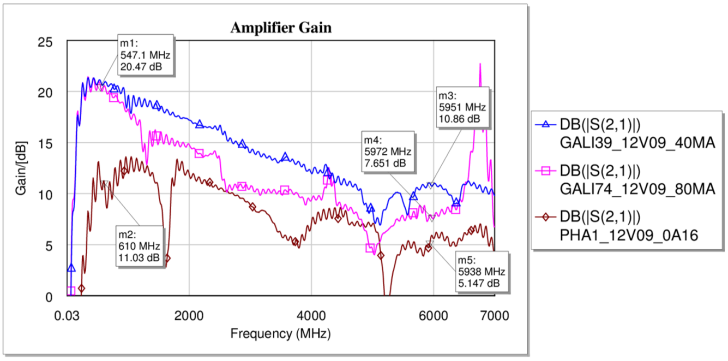

Figure 20: Measured S21 transmission parameters for the three aforementioned amplifiers: the Gali-39+ (blue), the Gali-74+ (pink), and the PHA-1+ (brown).

Figure 20 shows the gain of the amplifiers as a function of frequency. We can see that the gain of the amplifiers is significantly ($\sim 5dB$) less than the gains predicted by the data sheets. This might be attributed to lossy components or an impedance missmatch caused by moving the reference design from one pcb dielectric to another. Using the spectrum analyzer functionality of the field fox, we observed the output spectrum of the amplifier and determined that no oscillations were occurring (Figure 21).

3.2 Other components

Two additional "helper" circuits were built and are shown in Figure 22.

4 Results

Once all the individual components had been assembled, tested, and characterized individually, they were slowly amassed into transmit and receive signal chains. These chain sub-assemblies were tested with a variety of tools to ensure that they would work when cascaded together.

This was incredibly important because although all devices are nominally matched to 50 ohms, many devices will not function if the match isn't close enough. For example, when the oscillator,

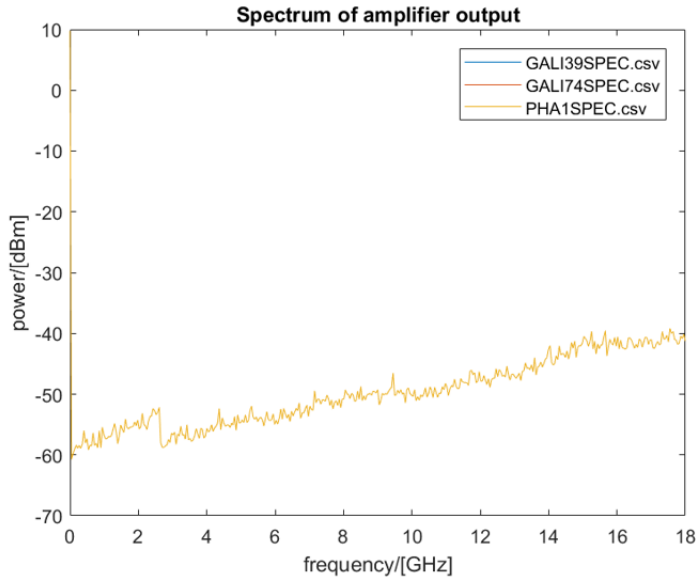

Figure 21: Output spectra of the three amplifiers. No oscillations observed.

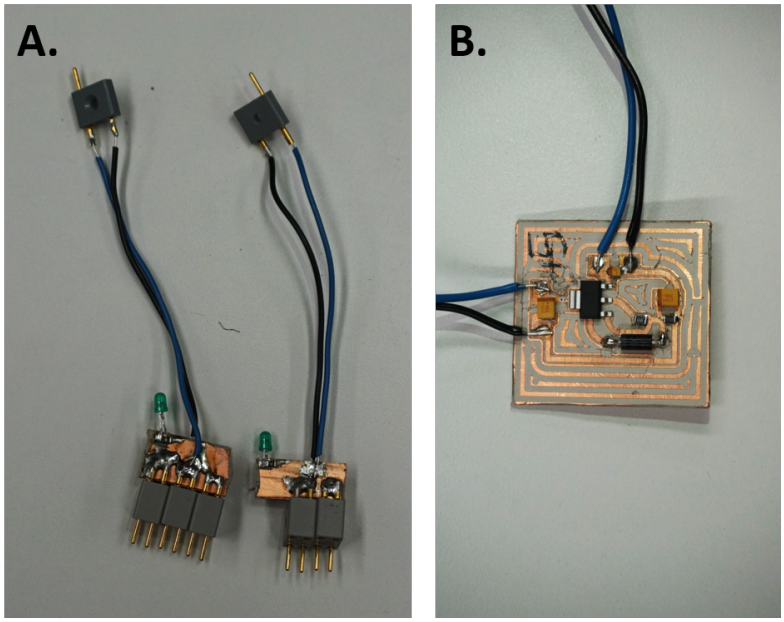

Figure 22: Power distribution circuit shown in (A) note the status LED. Linear regulator boards provided 5V for the vco (board included a trimpot for Vtune) and 2.15V for the custom oscillator.

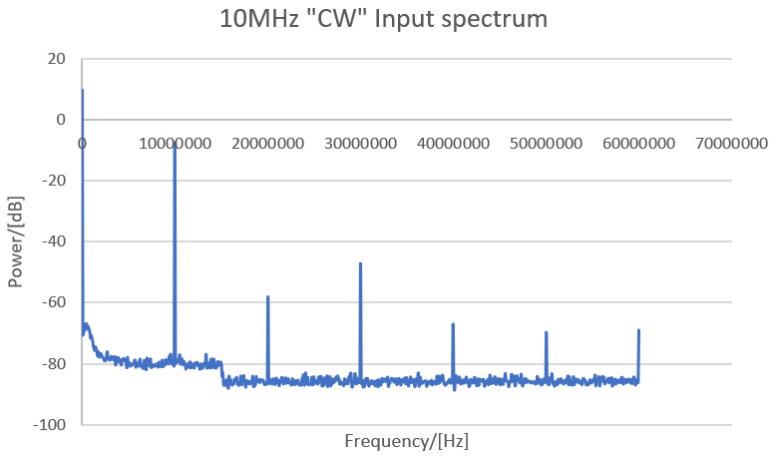

Figure 23: Frequency content of the 10MHz sine wave which was up-converted and transmitted across the radio link.

which worked perfectly by itself, was connected to the hybrid mixer, which also worked perfectly in prior tests, in an up-converting application, the signal coming from the RF port looked nothing like our IF input. Eventually, it was realized that the impedance match of the balanced mixer to the oscillator was likely the cause of the issues and a buffering amplifier (followed by an attenuator) was introduced to desensitize the oscillator to the impedance miss-match from the mixer and ultimately deliver the performance that we needed.

The final transmit and receive signal chains are shown in Figure 24B and A respectively.

For many of these tests, we used a signal generator to produce a -6dBm tone at 10MHz which acted as a stand-in replacement for the FM modulated signal. The frequency spectrum of this 10MHz signal is shown in figure 23.

Figure 25 shows the frequency spectrum of the transmitted signal immediately before arriving at the antenna. As expected, we see a very large leak-through signal at the oscillator frequency (From our previous tests, we can expect leakage of around -20dB) and a number of side-bands which are the 10 MHz signal and its harmonics. The transmit power of the 10MHz signal is around 0dBm while the power of the main 5.75Ghz tone was around 12dBm. These numbers are in close agreement with our predicted values. Given a 10MHz signal at -6dBm, a mixer with 15dB conversion loss, 4dB loss due to the pass band in the band-pass filter, and 25 dB of gain, we are left with exactly 0dBm at 10MHz.

Ultimately, we were able to successfully demonstrate the transmission of a range of frequencies from 5MHz to 10MHz at a distance of over 250 feet with a signal to noise ratio of over 70 dB[10]. The test setup for this measurement can be seen in Figure 26. Our transmit antenna and signal chain was setup on the far side of Moore while our receiver was placed at the edge of the grass nearest the parking lot. The received signal can be seen in Figure 27. For this particular test, the frequency of the IF transmission was 7MHz, although the RX figure shows that the signal has a frequency to 8.2MHz. The signal origin was verified by switching the IF signal on and off and blocking the antenna link. This offset is attributed to a difference in operating frequencies between the oscillator on the transmit side and the VCO on the receive side. These difference can come from many sources including from the instability in the oscillators themselves and from the dwindling voltage from our battery packs[11]

[10]Due to unforeseen shipping complications, we were unable to transmit an FM signal over our radio link

[11]When checked after our demonstration, we found that both 12V battery packs had final voltages around 7V

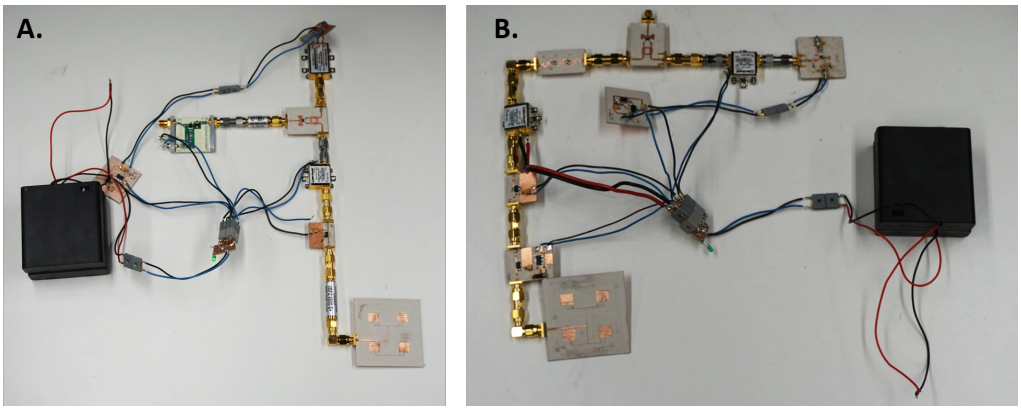

Figure 24: Transmit signal chain (B) and Receive signal chain (A).

Using the tiles on the ground, we estimated this distance to be in excess of 250 feet. At its maximum the received signal is around -25dBm which is in good agreement with the expected received signal strength at 250 feet. Given 0dBm transmit power, -65 dB due to 250feet of free space loss, plus 50 dB from amplification, and an additional 10dB of loss from the mixer, we should expect to see around -25dB of signal at the spectrum analyzer.

Given a noise floor of approximately -90dBm in our received signal, a "typical" signal to noise ratio of 26dB as quoted in the TEA5767HN FM receiver (that we would have used if we had more time)[12]. Our system might have had a maximum sensitivity of -64dBm. This roughly equates to roughly -25-(-64) = 39dB worth of margin. If taken at face value, this equates to an increase in our range by a factor of 100 or a final transmit distance of roughly 4 miles!

5 Limitations

While our project was highly successful, we were limited by several factors , and due to a lack of time, we were unable to optimize our radio to its full potential. If given more time, we would change the following things:

We struggled the most with matching the operating frequency of the voltage controlled oscillator to that of the custom "fixed" oscillator. It certainly didn't help that our batteries were depleted when we were testing. A poor power supply could certainly explain why the frequencies were drifting relative to each other.

In both the RX and TX chains, we could have added in additional gain to bolster our signal to noise ratio. For example, given that the OP1dB compression point of our last amplifier was chosen specifically to be higher than +20 dBm, we could potentially have added an additional 10dB of amplification with out driving the final amplifier into saturation (at the 5.8GHz LO tone).

Because we elected not to make any custom amplifiers, we always had a datasheet value for the noise figures of our amplifiers. However, it's possible that the PCB design could have changed those values so if we had more time, it would be nice to take more accurate measurements of the amplifier noise figures and cascade them in a more optimum way[13].

indicating that they had been completely exhausted.

[12] https://www.voti.nl/docs/TEA5767.pdf

[13] Amplifiers are currently cascaded according to noise figure reported in datasheets

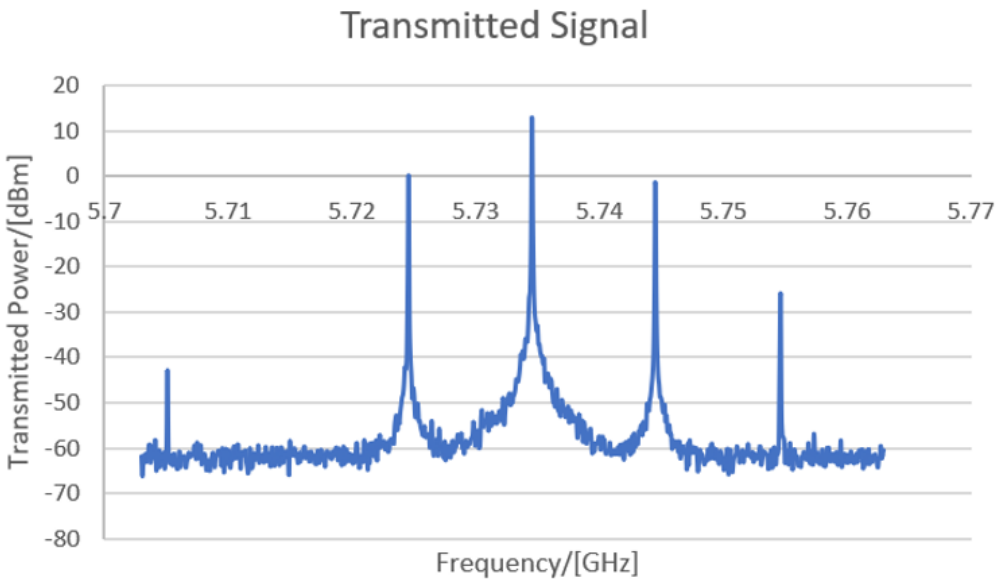

Figure 25: Frequency content of the transmitted signal immediately before being transmitted

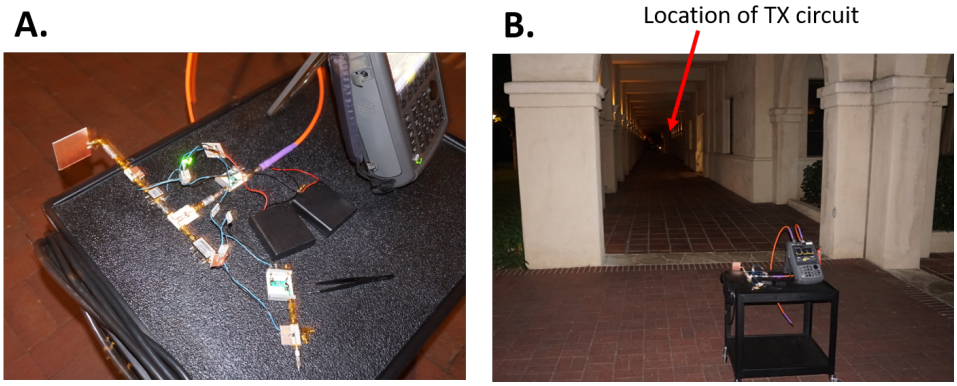

Figure 26: Receive chain as setup for testing outside Moore (A). Test setup used to determine the range of our signal (B).

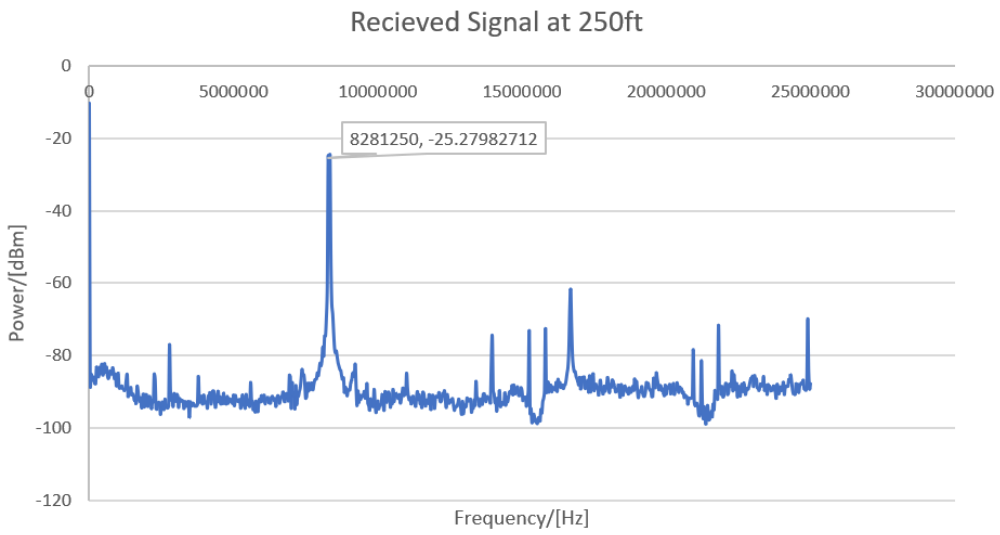

Figure 27: Frequency content of the received signal after being down converted from 5.8GHz. The signal should nominally be 7MHz, but due to oscillator drift and tuning errors, the final received signal was detuned by $\sim$ 1MHz

6 Conclusion

In this project we designed and built a working radio transmitter and receiver which was demonstrated to operate at a range of more than 250 feet with a signal to noise ratio of roughly 70dB. This project consisted of many moving parts of which we optimized and constructed 4 of them. In particular, we built two active components, a balanced mixer and an oscillator, as well as two passive components, a 5-segment coupled-line band-pass filter, and a 4-element patch antenna array. The mixer had a minimum conversion loss of around 10dB for down-conversion and 20dB for up-conversion. The oscillator was tuned to 5.75GHz and had an output power of around -3dBm. The band-pass filter had a bandwidth of 600MHz and a pass-band loss of 4dB. The patch array had a gain of 8.4dBi and a -3dB bandwidth of 50 degrees. This Project is certainly a fitting end to the term in that it allowed us to further explore many microwave concepts and furthered our knowledge of microwave technologies on a systems level – experience that will certainly prove useful down the road.

Appendix

```
import numpy as np
import os

def to_complex(r, th):
        th = th*3.1415926/180
        return r*(np.cos(th)+np.sin(th)*1j)

def angle2(th):
        return np.angle(th)*180/3.1415926

for jj in os.listdir(os.getcwd() + '\\in'):
        print jj
        f = open('in/' + jj)
        out = open('out/' + jj[:-3] + 's3p', 'w')
        out.write('!3-port S-parameters\n')
        out.write('%s %s %s %s %s %s\n' % ('#', 'MHz', 'S', 'MA', 'R', '50'))
        end_data = 0
        end_head = 0
        for line in f:
                if line[0] == '!' or line[0] == '#' or line[0] == '\n':
                        if end_head == 1:
                                end_data = 1
                        end_head = 0
                        continue
                elif end_head == 0:
                        end_head = 1
                if end_data:
                        continue

                data = [float(x) for x in line.split(' ') if x != '']

                s11 = to_complex(data[1], data[2])
                s21 = to_complex(data[3], data[4])
                s12 = to_complex(data[5], data[6])
                s22 = to_complex(data[7], data[8])

                zeta = s11 + s21 + s12 + s22

                d11 = 1 - s11 - s12
                d12 = 1 - s11 - s21
                d21 = 1 - s12 - s22
                d22 = 1 - s21 - s22

                s11 += d11*d12/(4-zeta)
                s12 += d11*d21/(4-zeta)
                s13  = 2*d11/(4-zeta)
                s21 += d22*d12/(4-zeta)
                s22 += d22*d21/(4-zeta)
```

```
s23   = 2*d22/(4-zeta)
s31   = 2*d12/(4-zeta)
s32   = 2*d21/(4-zeta)
s33   = zeta/(4-zeta)

out.write('%d %f %f %f %f %f %f\n' % (int(data[0]), abs(s11), angle2(s1
out.write('\t %f %f %f %f %f %f\n' % (abs(s21), angle2(s21), abs(s22),
out.write('\t %f %f %f %f %f %f\n' % (abs(s31), angle2(s31), abs(s32),
```

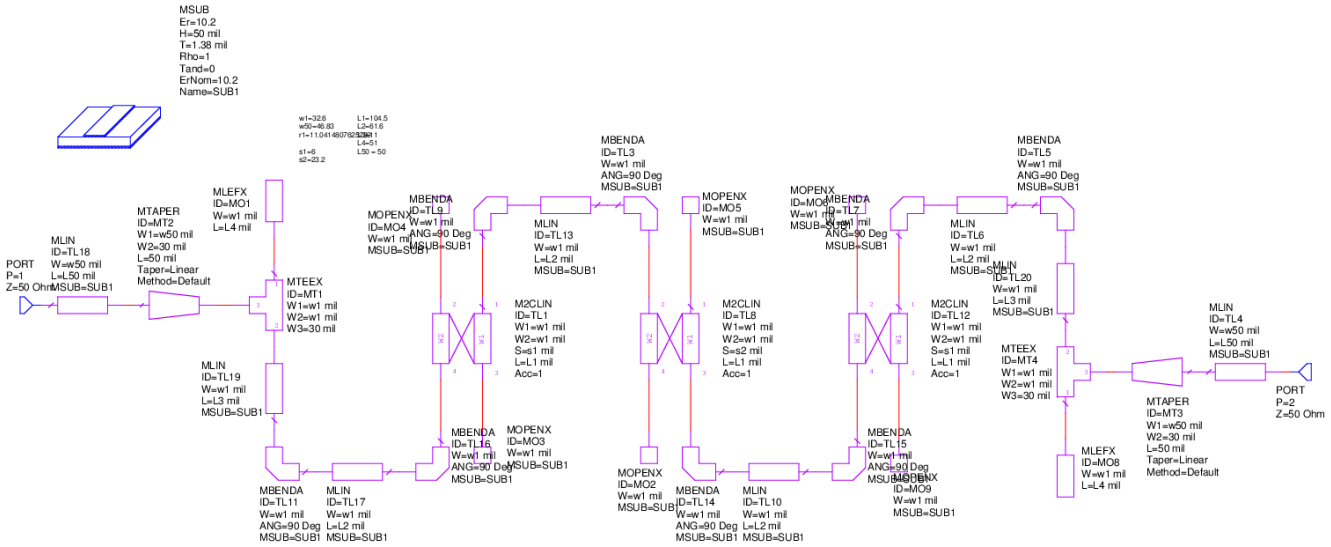

Figure 28: 3-segment bandpass filter as implemented in MWO.

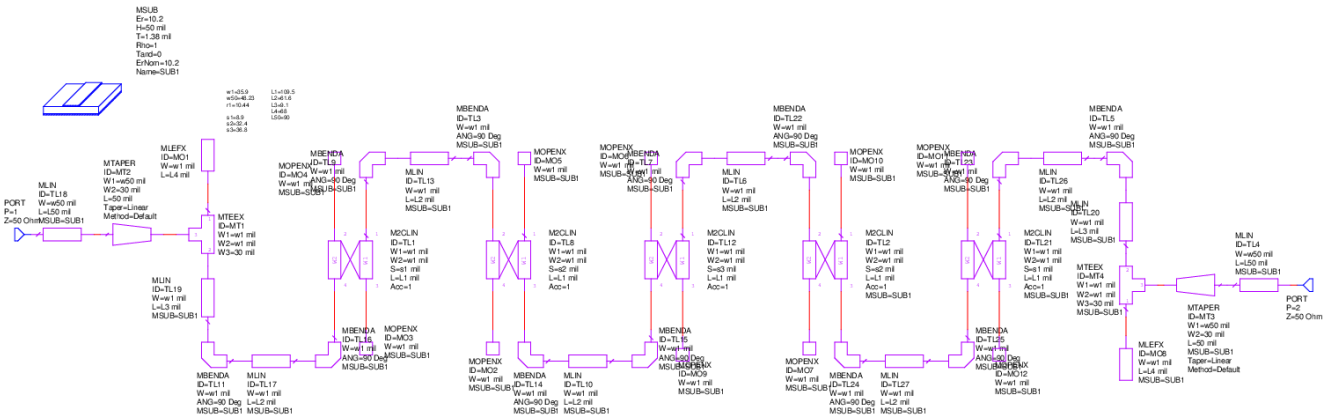

Figure 29: 5-segment bandpass filter as implemented in MWO.

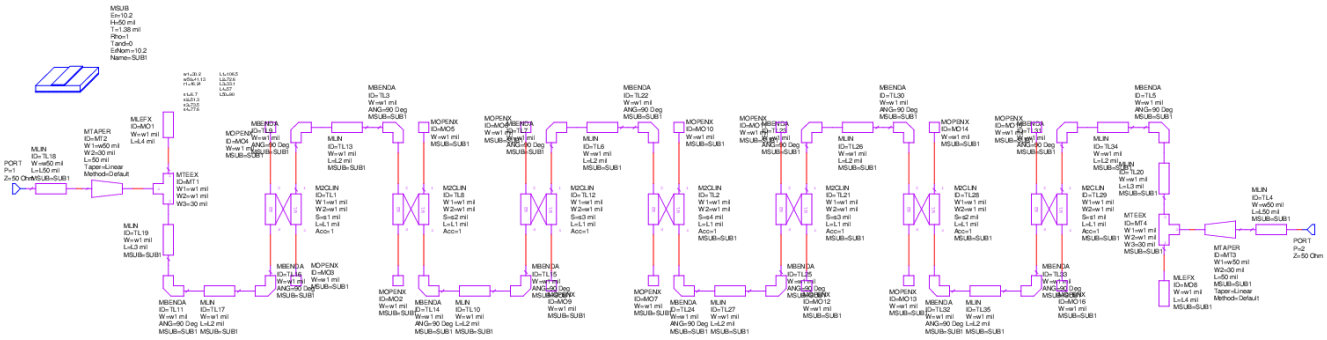

Figure 30: 7-segment bandpass filter as implemented in MWO.

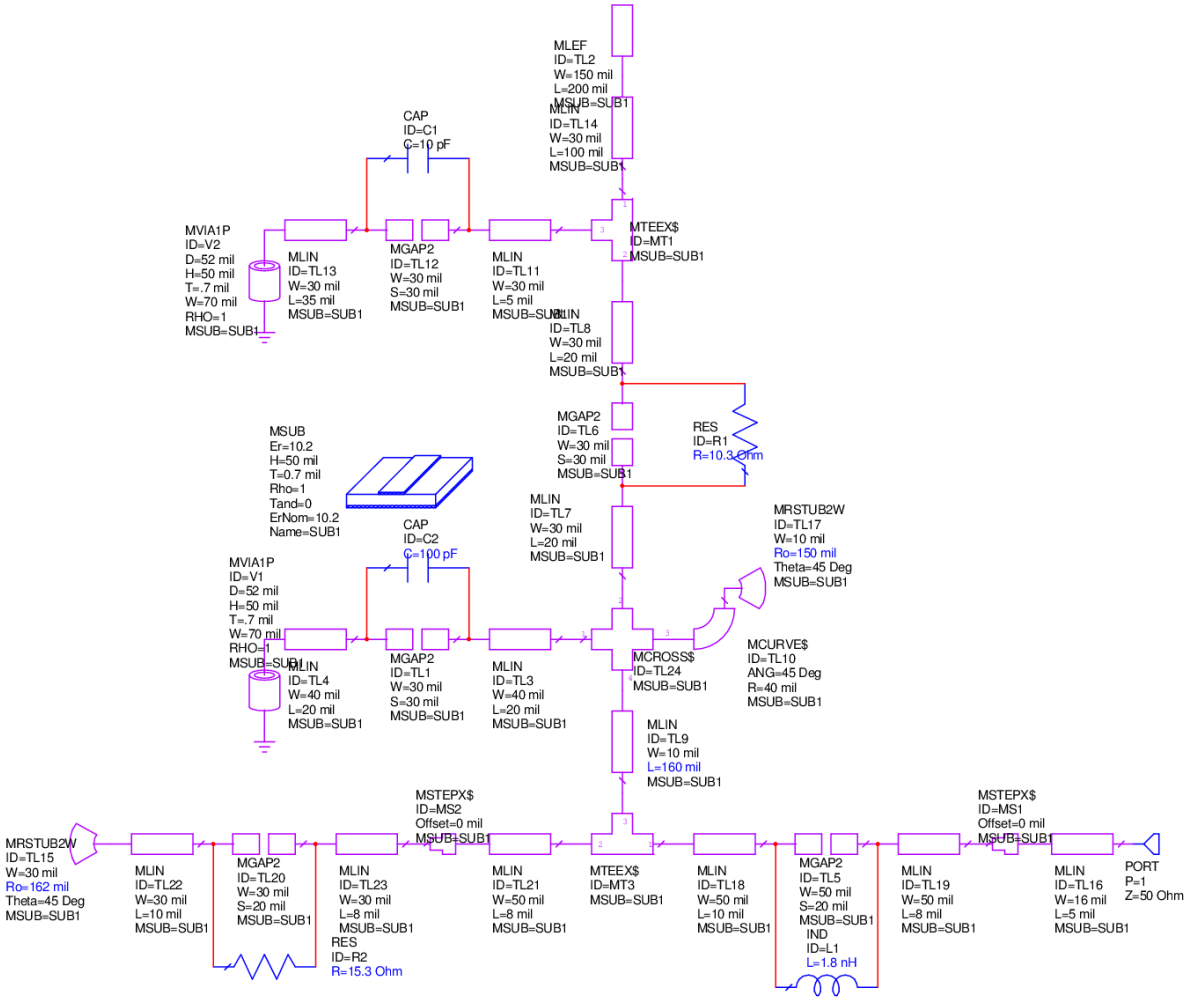

Figure 31: Collector network. Designed to give a real impedance equal to 1/3 the real impedance looking into collector of transistor and a conjugate match to the imaginary impedance of the transistor.

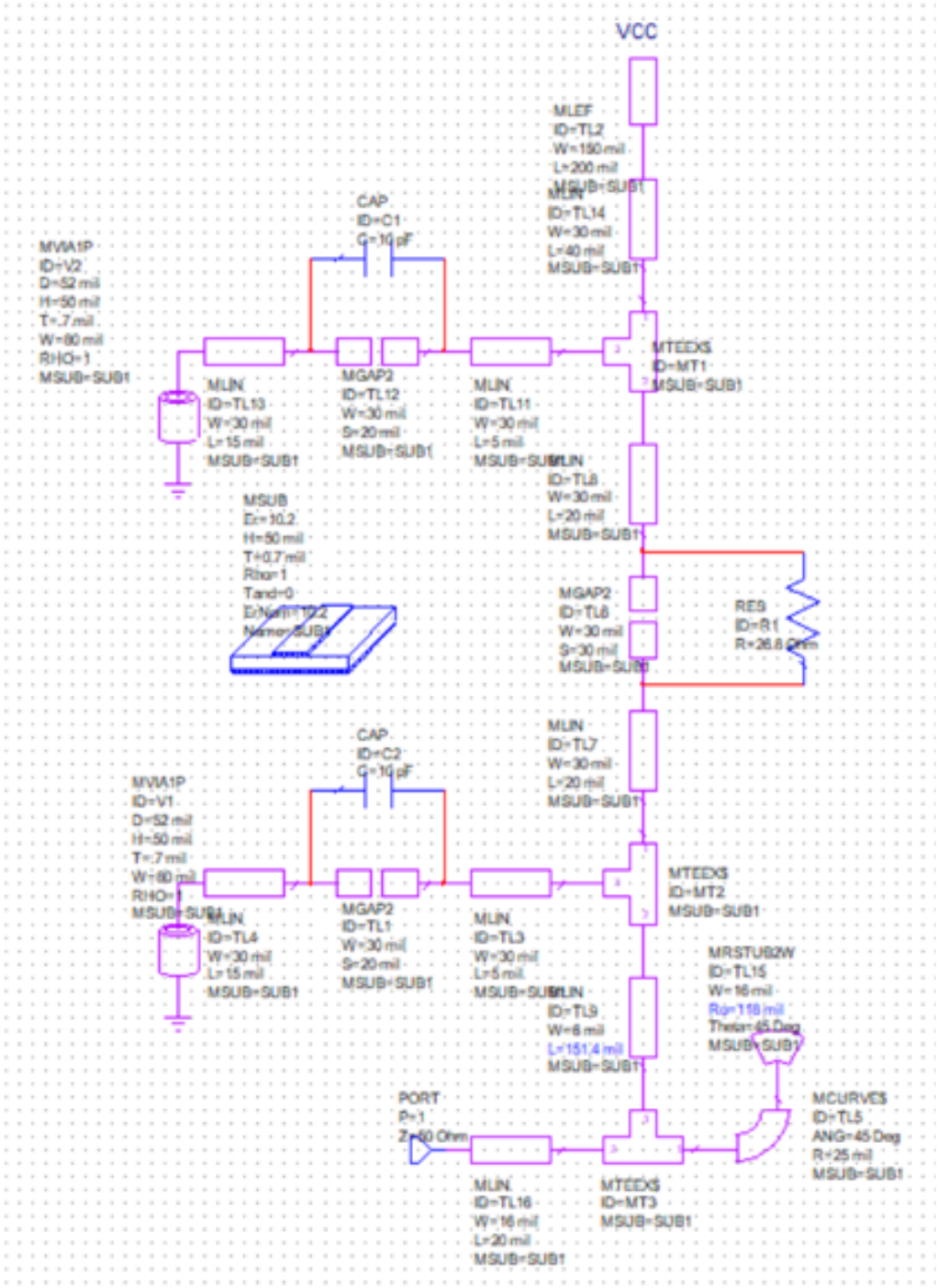

Figure 32: Final circuit for the base network as designed in microwave office. Network provided proper biasing with 26 $K\Omega$ resistor.

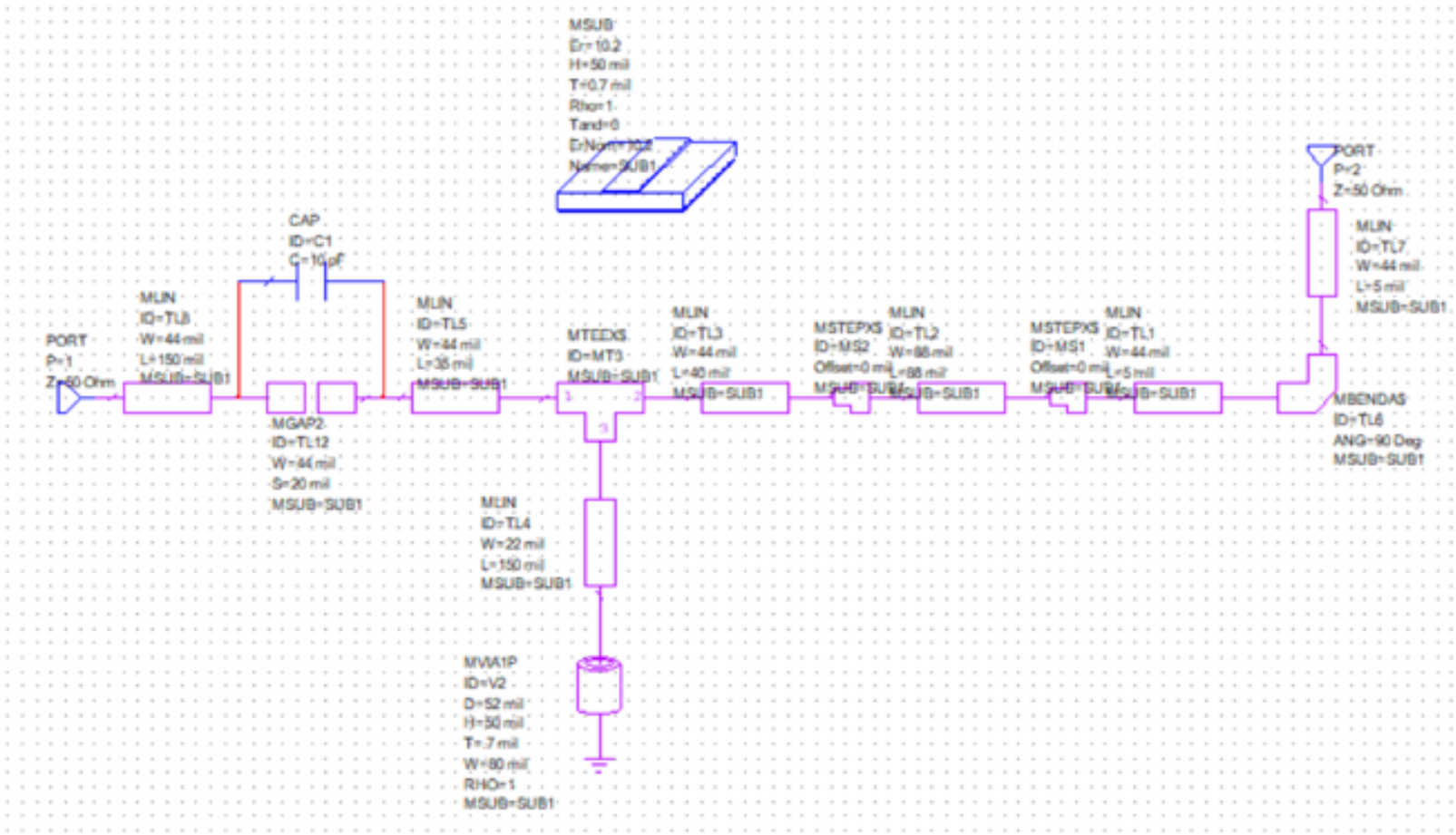

Figure 33: Output network as designed. Network designed to pass the oscillation frequency tones while also providing a path to ground.

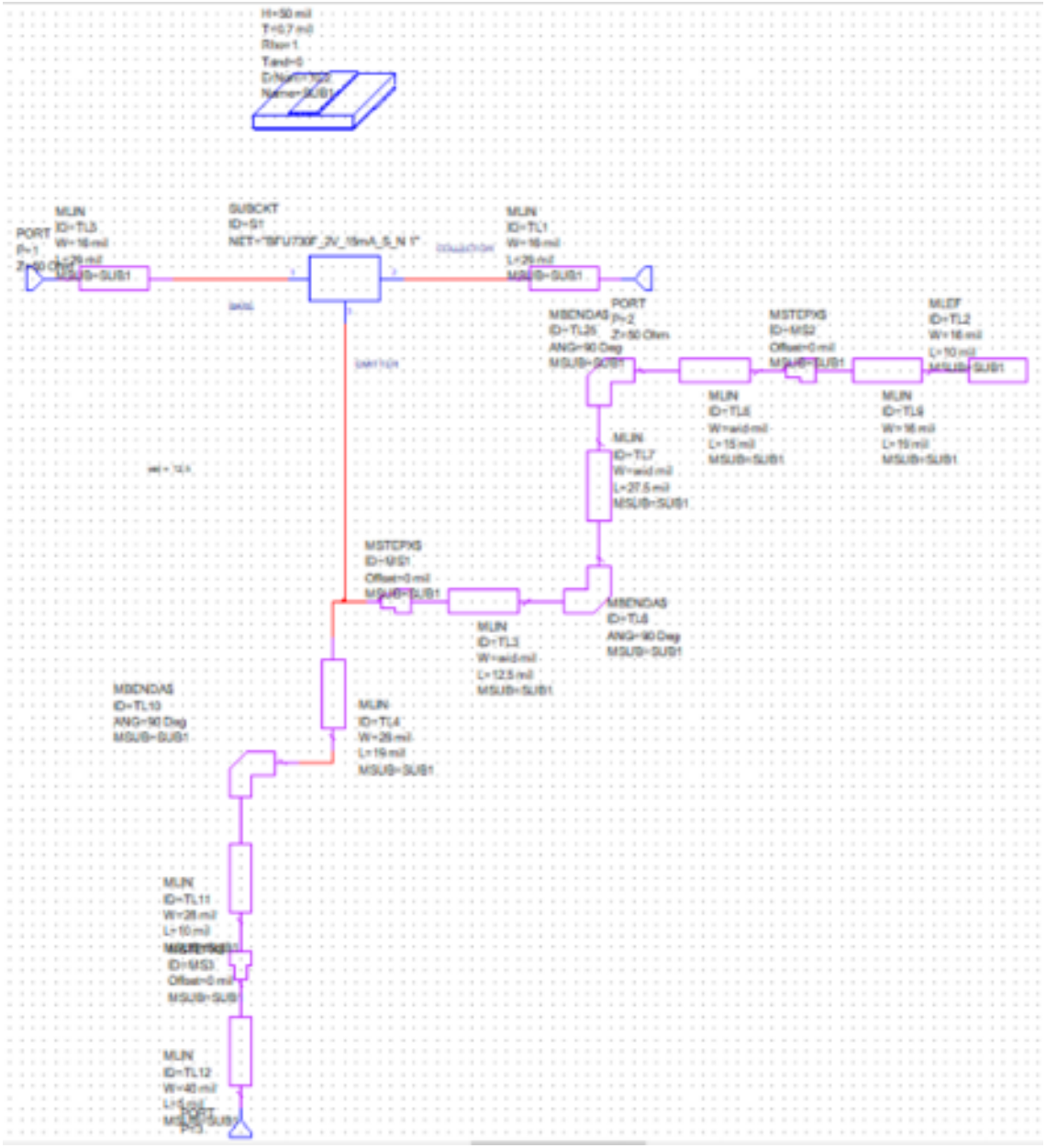

Figure 34: Footprint of the BFU730 Transistor as implemented in MWO. Transistor .S3P model included for simulations.

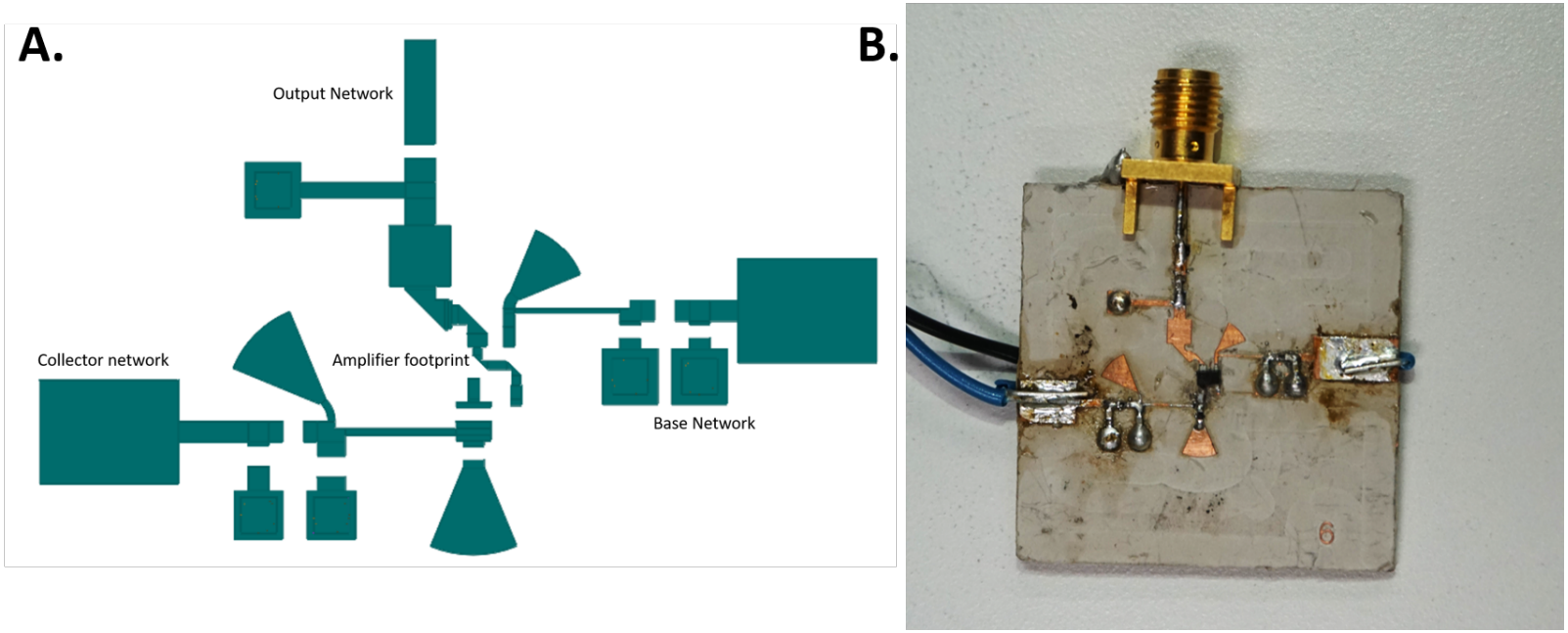

Figure 35: Layout of Oscillator circuit as designed in MWO (A) and as fabricated (B).

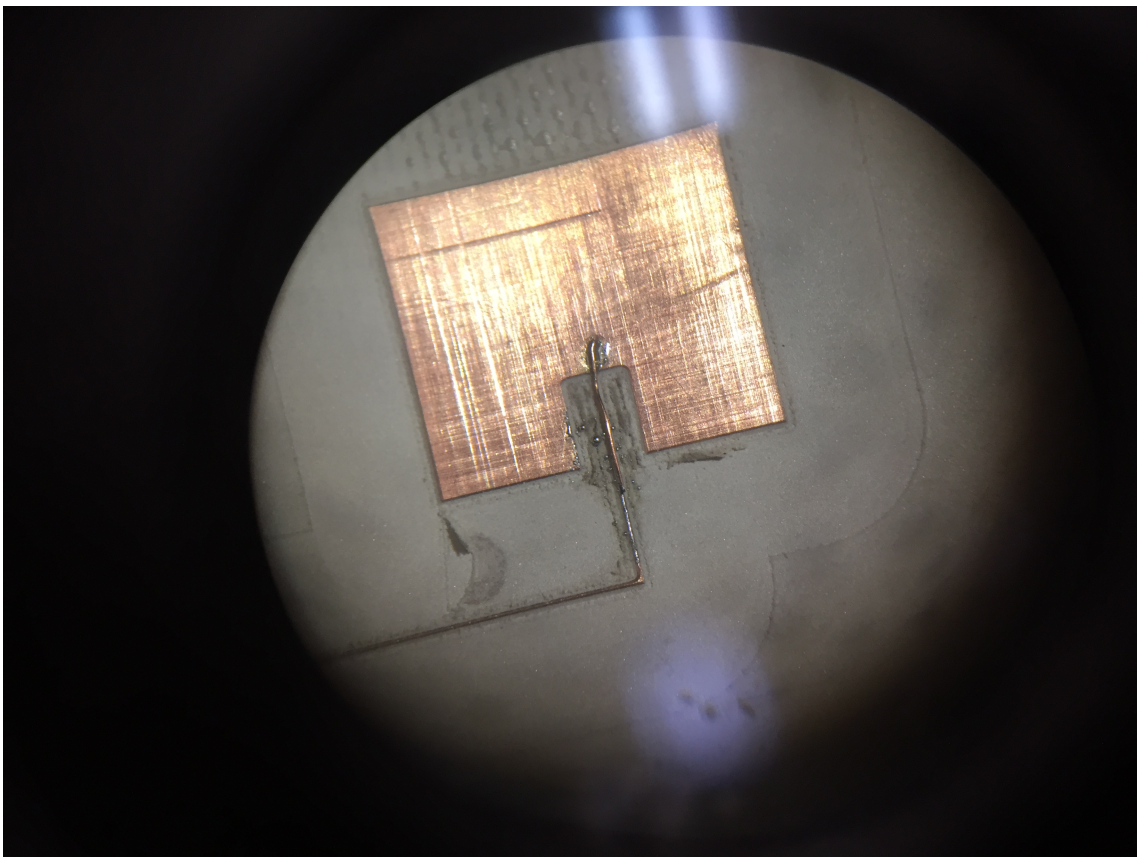

Figure 36: During fabrication of 4-element patch array, several of the 100ohm (7 mil) traces were severed during the milling process. These were fixed by using a single strand of copper wire from a solder wicking braid.